On the Motion of Fluidized Granular Currents: Motion Along Horizontal Surfaces

David E. Jessop[*]   M. A. Gilbertson[†]

A. J. Hogg[‡]

[*]University of Bristol, d.e.jessop@bris.ac.uk

[†]University of Bristol

[‡]University of Bristol

Jessop et al.: Horizontal motion of Granular Currents

ON THE MOTION OF FLUIDISED GRANULAR CURRENTS: MOTION ALONG HORIZONTAL SURFACES

By D. E. JESSOP [1,2] , M. A. GILBERTSON [2] & A. J. HOGG [1]

[1] Department of Mathematics, University of Bristol, Bristol. BS8 1TW

[2] Department of Mechanical Engineering, University of Bristol, Bristol. BS8 1TW
Corresponding author: d.e.jessop@bris.ac.uk

ABSTRACT

The motion of fluidised granular currents over horizontal surfaces is investigated experimentally and by mathematical modelling of solid and fluid phases. Analytical solutions for the bulk motion were tested by experiments involving material being introduced at a constant volume flux, and a reasonable agreement found between theoretical predictions and laboratory measurements.

INTRODUCTION

Aerated granular flows are a feature of large scale and destructive natural hazards that arise from volcanism as pyroclastic flows and phenomena such as avalanches and landslides. They are also utilised in industrial processes where the bulk transport of powders is required in order to produce pharmaceuticals, agricultural materials and foodstuffs. An understanding of the underlying physical processes that control these flows is necessary to avoid or avert disasters and increase efficiency of these industrial processes.

Fluidised beds and the apparatus used in this investigation incorporate a porous base that allows a flow of gas initially perpendicular to the base to permeate through the overlying (granular) material. The presence of this gas flow exerts a drag on particles that constitute the material and supports part, or all, of their effective weight.

Flows of 'dry' granular material propagating over horizontal and inclined surfaces have been treated extensively in the literature (see, for example, Savage & Hutter (1); Balmforth & Kerswell (2); Pouliquen & Forterre (e3)). Often the granular material is released from rest behind a lockgate that is rapidly removed to initiate the flow, or the material is introduced continuously at a particular point and flows rapidly away before undergoing a deceleration phase. We consider only the latter case in this paper. As frictional forces between particles as well as basal friction are responsible for this rapid attenuation, disruption of force chains transmitting stress between particles by fluidisation suggests an increased mobility for fluidised granular flows (Roche *et al.* (4)).

In this paper we aim to develop a framework within we may begin to understand some of the complex physics associated with fluidised granular flows of all scales.[1]In

order to do this we first discuss the forces and interactions associated with each phase,giving separate mass and momentum conservation equations for both. Next we explore simplifications that can be made for flows along horizontal surfaces and look for analytical solutions to the resulting equation of motion. Then we describe the experiments that were performed and analyse the resulting data with a view to evaluating our assumptions. Finally we give conclusions of the work.

THEORY

Background & assumptions

We consider a two-dimensional flow of a granular material over a horizontal surface. The flow is thin so that its horizontal length scale, L, far exceeds typical values for its thickness, H. The material is also assumed to be fully fluidised so that the weight of the solid phase is entirely balanced by the drag from the imposed gas flow; there are no residual stresses or particle pressures within the solid phase, nor are particle-particle interactions become important. This assumption is justified from considering Appendix A in Eames & Gilbertson (6). Thus, as in figure 1, orientating the x and z coordinate axes to be horizontal and vertical, respectively, and denoting the voidage of the material by ε, the density of the solid phase by ρ_s and gravitational acceleration by $-g\hat{\mathbf{z}}$, this balance is given by

$$0 = \mathbf{f}_{fs} \cdot \hat{\mathbf{z}} - (1-\varepsilon)\rho_s g, \tag{1}$$
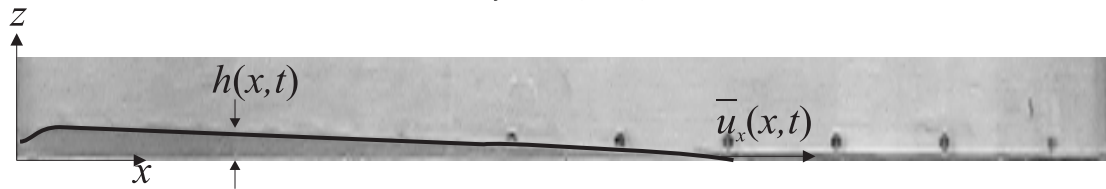

Figure 1. Orientation of axes, and notation associated with modelling the currents. The image shows a fluidised current approximately 65cm long and 2cm thick. An outline has been drawn on the surface of the flow for clarity

where $\mathbf{f}_{fs}$ is the bulk drag force between the fluid and solid phases. Since the flow is thin, vertical fluid accelerations are negligible and thus the pressure gradient in the fluid phase must also balance the weight of the fluid and the drag between the phases. Thus denoting the fluid pressure and density by p_f and ρ_f

$$0 = -\frac{\partial p_f}{\partial z} - \mathbf{f}_{fs} \cdot \hat{\mathbf{z}} - \varepsilon \rho_f g \tag{2}$$

Thus from (1) and (2) we deduce that the fluid pressure is hydrostatic and given by $p_f = \big((1-\varepsilon)\rho_s + \varepsilon\rho_f\big)g(h-z)$ where h is the height of the material surface.

The imposed interstitial gas flow plays a crucial role in fluidised systems and in our model it is represented through the drag term $\mathbf{f}_{fs}$. We model this using the Ergun equation (see Rhodes (5)) given by

$$\mathbf{f}_{fs} = \frac{150\mu_f(1-\varepsilon)^2}{d_p^2\varepsilon^3}(\mathbf{u}-\mathbf{v}) + \frac{1.75\rho_f(1-\varepsilon)}{d_p\varepsilon^3}|\mathbf{u}-\mathbf{v}|(\mathbf{u}-\mathbf{v}). \tag{3}$$

where μ_f is the viscosity of the gas, d_p is the particle diameter, $\mathbf{u}$ and $\mathbf{v}$ are the gas and solid velocities, respectively. In this report we chose to write the z component of the gas velocity as the sum of the imposed gas speed, u_{gi} and the motion induced by the presence of particles u_z, or $\mathbf{u} = \left(u_x, u_z + u_{gi}\right)$. Ignoring numerical factors, the ratio of the two terms in the Ergun equation is equivalent to a Reynolds number for the gas flow through the fluidised bed, Re_{bed}; typical values for physical parameters in the experiments reported later give this to be $O(1)$ so the flow through the bed is laminar and only the left hand term of (3) is considered during the analysis. To ease writing, we combine the group of constants multiplying the difference in velocities as $K = 150\mu_f(1-\varepsilon)^2/d_p^2\varepsilon^3$ and thus we approximate $\mathbf{f}_{fs} = K(\mathbf{u} - \mathbf{v})$.

We now consider the horizontal components of the momentum equations for each phase. In general these could include the inertia of each phase, stream-wise pressure gradients, resistive forces and contributions from the inter-phase drag law. In this paper we assume that inertia is negligible. This requires that the reduced Reynolds number is small, given by

$$R = a^2 \mathrm{Re} \ll 1$$

where a is the aspect ratio of the flow ($a = H/L = O(0.01)$) and $\mathrm{Re} = \rho_s UH/\mu$, where $U = O(10)$ cm/s and μ^{1} are a velocity scale and the effective viscosity respectively. This gives $R = O(0.01)$. Observations made during laboratory experiments suggest that the flows are not inertially driven. For instance, if the flow rate of gas into the apparatus is shut off, the flow of material stops instantaneously. This behaviour is in agreement with Eames & Gilbertson (6) who observed steady flows and concluded that fluidised granular flows propagate in a similar manner to a viscous fluid as described by Huppert (7).

Experiments performed with rotating paddle viscometers such as those performed by Matheson *et al.* (8), Furkawa & Ohmae (9) and Schügerl *et al.* (10) using a fluidised bed contained within two concentric cylinders all agree in giving the observed viscosity of fully fluidised beds to be in the range of 0.05 to 2Pas. Caution must be paid to these results, however, as along with 'viscous' losses there is an associated momentum loss due to the acceleration of the particles. Furthermore, the results of such experiments are only valid for low applied shear gradients as the particles have a tendency of migrating to the outside of the cylinder/paddle due to their inertia thus creating a non-homogeneous suspension. This does suggest, however, that the viscosity of a suspension of particles is somehow altered.

On this assumption of negligible inertial effects we find that the horizontal component for the solid phase is given by

$$0 = K\left(u_x - v_x\right) \tag{4}$$

thus implying the horizontal gas and solid velocities are identical. For the fluid phase we find that

$$0 = -\frac{\partial p_f}{\partial x} - K\left(u_x - v_x\right) + \frac{\partial \tau_{xz}}{\partial z} \tag{5}$$

---

[1] A value for μ will be derived in the RESULTS section

where τ_{xz} is the shear stress within the fluid phase. We propose that $\partial \tau_{xz}/\partial z$ scales as u_x/h^2 as it would for a viscous fluid with a constant of proportionality of the same dimensions as viscosity: we take this to be the mixture viscosity. As shall be discussed later, we assume that ε is constant. Upon integration of (5) and substitution into the depth integrated mass conservation equation for the solid phase, we obtain the governing equation for evolution of the height profile

$$\frac{\partial h}{\partial t} = \frac{(1-\varepsilon)\rho_s + \varepsilon\rho_f}{3\mu} g \frac{\partial}{\partial x}\left(h^3 \frac{\partial h}{\partial x} \right),\tag{6}$$

which can be solved numerically subject to the boundary conditions $h(x_f) = 0$ and $v_x h|_{x=0} = q$ where x_f is the front position and q is the volumetric flux of material. The total volume of material at any time is given by

$$\int_0^{x_f} h\, dx = q\, t.\tag{7}$$

Analytic solutions

Huppert (7) obtained an equation of the same form as (6) and was able to construct similarity solutions subject to an identical condition as (7). We follow the same method (see also Barenblatt (11)) to obtain the following solutions in terms of the similarity variable, ξ and similarity solution $H(\xi)$

$$x(t) = \left(\Lambda q^{3/4} t \right)^{4/5} \xi,\tag{8}$$

and

$$h(x,t) = \left(q^2 t/\Lambda \right)^{1/5} H(\xi),\tag{9}$$

where $\Lambda = \left((1-\varepsilon)\rho_s + \varepsilon\rho_f \right)g/3\mu$. Normalising (8) with respect to the front position, x_f so that $y = \xi/\xi_f$ and substituting (9) into the governing equation (6) leads, after rescaling, to the following non-linear ODE in $H(y)$

$$H^3 H'' + 3H^2 \left(H'\right)^2 + 4/5\, yH' - 1/5H = 0.\tag{10}$$

where a prime denotes differentiation with respect to y. $H(y)$ and ξ_f can be found numerically, subject to knowing Λ, allowing us to find x_f.

EXPERIMENTAL SETUP

To test the hypotheses made in the previous section a series of experiments was devised wherein material is introduced at a constant flux. These are similar to the experiments performed by Eames & Gilbertson (6) except on a much larger scaleso that data series over sufficiently long time scales could be obtained. The apparatus used was designed specifically for this investigation. An image of it is shown in figure 2. To avoid possible electrostatic effects which have arisen with perspex walled fluidised beds, glass was used for the front and 15mm thick aluminium plate for the back and sides. This has the advantage of being rigid and thus ensuring that the channel in which material flows is straight throughout its length.

A basal distributor plates made from a 'sandwich' of porous Vyon D sheets from

Porvair Ltd. surrounding a layer of Geldart A particles ranging from 45-90 μ m. This causes a large pressure drop so that the gas flow is constant along their length and that the presence of particles above the distributor plates does not locally affect the gas supply.
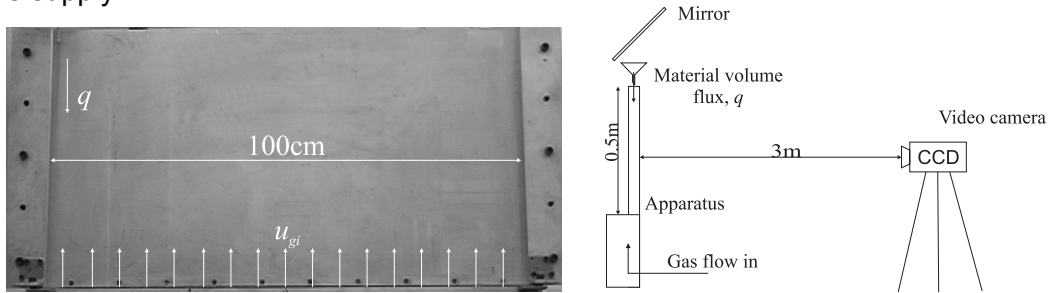
Figure 2. a) (*left*) Front view of the apparatus. b) (*right*) Schematic of the experimental set up.

Experiments were recorded using a digital camera. As the apparatus is quite long a wide camera angle must be used in order to capture the flows in their entirety. It was found to be easier to determine the position of the front by viewing the flows from above; at the same time it is desirable to see how the height profile evolves. To resolve these issues a mirror was positioned above the apparatus as is shown in figure 2b so that both could be recorded simultaneously. Data extraction was done by viewing still images taken from the videos using the UTHSCSA ImageTool programme. Assuming that the front position can be determined from an image to within a few pixels and the 100cm length of apparatus equates to something in the order of 450 pixels, then we estimate the error in our measurements to be $O(1)$ cm. This is accounted for as error bars of this magnitude in the plots of data in the next section.

The particles used were glass spheres in the range of 250-500 μ m (Potters Ballotini grade C) corresponding to a Geldart B powder. Before starting any experiments, the powder was conditioned by vigorous fluidisation. Viewing the experiments from above presented the problem that the slightly off-white particles were hard to distinguish from the white Vyon sheet. To ease visualisation they were coloured using very dilute artists acrylic paint and then dried thoroughly to leave only the pigment. Using particles of this size ensured non-cohesive behaviour. Bed expansion using these particles is negligible so we assume that ε is constant for all values of u_{gi} used in the experiments.

Standard fluidisation curves were constructed using data for the pressure drop through various bed heights from independent experiments (as described in Davidson & Harrison (12); Rhodes (13) etc.) from which the minimum fluidisation velocity, u_{mf} was found to be 10.78cm/s. This is in agreement with theoretical predictions made by equating the first term from the Ergun equation (3) with the bed weight per unit volume: for the smallest size of particles this gives $u_{mf} = 5.854$cm/s whilst for the largest size of particles $u_{mf} = 23.416$cm/s.[2]

---

[2] physically parameters used were $\rho_s = 2500$kg/m^3, $g = 9.81$m/s^2,

RESULTS

We expect from (8) that $x_f \sim (q^3 t^4)^{1/5}$. With knowledge of the constant Λ it should be possible to predict accurately the position of the front at any point in time. There is, however, at least one physical variable in Λ that is not well defined, namely the mixture viscosity, μ. This should be some function of ε, but the exact relationship is not currently clear. The voidage itself may also be hard to measure for any given experiment due to bed expansion. However, for not too high values of u_{gi}, we assume that ε is close to that measurable when unaerated. Instead we chose to try to collapse the data onto a single curve by scaling the front position with $q^{3/4}t$ so that

$$x_f = A\left(q^{3/4}t\right)^n, \tag{11}$$

where A and n are constants to be determined. Comparing this with (8) shows clearly that if n is in the region of 4/5 then our model is likely to be valid. Also A is related to Λ and we may hence be able to find a value for the mixture viscosity. The front propagation data is shown in figure 3a, and then as a function of $q^{3/4}t$ in figure 3b.
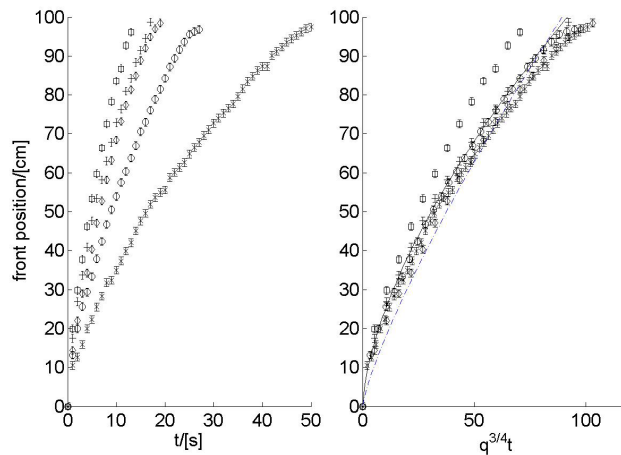

Figure 3. a) (*left*) Front position, x_f as a function of time, t for different volume fluxes of material and gas flow rates: $q =$ 2.544cm^2/s, $u_{gi}/u_{mf} = 1.3$ (x); $q = 5.2$cm^2/s, $u_{gi}/u_{mf} = 1.3$ (o); $q = 9.515$cm^2/s, $u_{gi}/u_{mf} = 1.3$ (<>); $q = 9.515$cm^2/s, $u_{gi}/u_{mf} = 1.48$ (+); $q = 9.515$cm^2/s, $u_{gi}/u_{mf} = 1.86$ ([]). b) (*right*) The same data for x_f but scaled with $q^{3/4}t$. Also plotted is a best fit curve (—) according to (11) using $A = 5.701$ and $n = 0.634$ and the curve predicted by (8) (— - —) with $A = 2.75$ and $n = 0.8$

Figure 3 shows the data points collapse well for all the experiments except when the

---

$\mu_f = 1.862 \times 10^{-5}$ Pas. ε_{mf} was taken to be 0.4 and the density of air was neglected.

values of u_{gi}/u_{mf} are particularly high. When at such high gas flow rates, the
powder bubbles vigorously which may alter the mechanisms that transport powder
within the bulk; otherwise particle movement was as a bulk motion.

Fitting a curve through all the data, we find that $A = 5.701$ and $n = 0.634$. We
observed a section of the distributor plate that might not be delivering the same flow
rate of gas as along the rest of its length. As this only accounted for the last 10cm of
the apparatus, it is reasonable to simply ignore the motion over this part.
Furthermore, it takes a little time for the flow to become fully developed and enter the
intermediate asymptotic regime that gives rise to the similarity solutions. With this in
mind, the data points corresponding to the first 30cm and final 10cm of the
apparatus were ignored and another curve fitted to the remaining data. This gave
$A = 5.225$ and $n = 0.659$. Both values are a little short of the 4/5 power we might
have expected.

Figure 4 displays new data from our experiments along with those of Eames &
Gilbertson (6). Using (11) with $n = 0.8$ seems to best fit their data whilst none of the
curves seem to fit our data. On being introduced to the apparatus, the material free
falls 0.5m before encountering the distributor plate[3]. Its kinetic energy causes it to
scatter forwards which clearly affects the results at such a short time and accounts
for the deviation of our data from that of Eames & Gilbertson (6). The flows were
certainly not fully developed and hence not in the intermediate asymptotic regime
meaning that similarity solutions do not apply here, so we should not expect any of
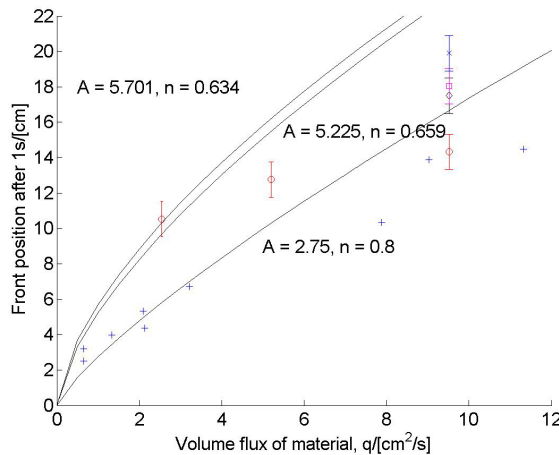the curves to fit the new data.

Figure 4. Front position after 1s as a function of the volume flux of material. Data from
Eames & Gilbertson (6) (+) where $u_{gi}/u_{mf} = 1.26$ is plotted along with our own data
for ratios of 1.3 (O), 1.48 ($\diamond$), 1.67 ([]), & 1.86 (x) respectively and lines
corresponding to (11) for various values of A and n.

Comparing (9) and (11) gives $\Lambda = \left(A/\xi_f \big|_{\alpha=1} \right)^{1/5} = 3779.56$ for $A = 5.225$.
Rearranging and using the values stated earlier in this paper gives $\mu = 0.0129$ Pas.

---

[3] This is compared to about 20cm in the case of Eames & Gilbertson (6)

CONCLUSIONS

We have presented data on the propagation of fluidised granular currents for several values of material volume fluxes and ratios of u_{gi}/u_{mf} for Geldart B powder in the range of 250-500 μ m. The minimum fluidisation velocity was determined by independent experiments to be 10.78cm/s. Comparisons have been made to theoretical predictions by use of similarity solutions and a suggestion made for the value of a mixture viscosity by use of the data.

We have proposed a model that describes the mechanical interactions of gas and solid phases. On the laboratory scale there is no contribution from inertial terms subject to the reduced Reynolds number, R, being small. Using quantities defined and derived earlier in this report, we find that this group is $O(10^{-2})$ and so our analysis is valid. When considering large scale geophysical phenomena such as pyroclastic flows which motivate this study, the typical flow speeds are much larger and have thicknesses measurable in tens of metres, R will be considerably higher so inertia will be more important. Full scale flows will then probably require a different dynamical balance, however both cases will require a similar descriptionfor the mechanics within the flows.

A plot of the front position, x_f against rescaled time ($q^{3/4}t$) gives a power-law distribution whose exponent, $n = 0.66$. According to the theory presented we expect the exponent to be 0.8, although the experimentally determined value is not unreasonable.

Our model is mathematically identical to that determined by Huppert ([7]) for viscous fluids. We believe that this is because the flows are driven by stream-wise pressure gradients and retarded by stresses that scale as v_x/h^2. These are analogous to viscous stresses found in fluids. This gives rise to viscous-like behaviour in the fluidised granular flow. Using experimental and numerically determined values we find a value for the mixture viscosity to be $\mu = 0.0129$ Pas, which not too dissimilar to viscosities found by Matheson *et al.* ([8]), Furkawa & Ohmae ([9]) and Schügerl *et al.* ([10]).

ACKNOWLEDGEMENTS

REFERENCES

1.   Savage, S. B. & Hutter, K. (1989). "The motion of a finite mass of granular material down a rough incline." *J. Fluid Mech.*, 199, 177-215.
2.   Balmforth, N. J. & Kerswell, R. R. (2005). "Granular collapse in two dimensions." *J. Fluid Mech.*, pre-print copy.
3.   Pouliquen, O. & Forterre, Y. (2002). "Friction law for dense granular flows: application to the motion of a mass down a rough inclined plane." *J. Fluid Mech.*, 435, 133-151.
4.

Jessop et al.: Horizontal motion of Granular Currents

4. Roche, O. Gilbertson, M. A. Phillips, J. C. & Sparks, R. S. J. (2005). "Experimental study of gas-fluidized granular flows with implications for pyroclastic flow emplacement." *J. Geophys. Research*, pre-print copy.

5. Rhodes, M. (1998). *Introduction to Particle Technology*, chap. 4. Wiley.

6. Eames, I & Gilbertson, M. A. (2000), "The flow of aerated particles over a horizontal rigid surface.", *J. Fluid Mech.*, 424, 169-195.

7. Huppert, H. E. (1982). "Propagation of two-dimensional and axisymmetric viscous gravity currents over a horizontal surface.", *J. Fluid Mech.*, 121, 43-58.

8. Matheson, G. L. Herbst, W. A. & Holt, P. H. (1949). "Characteristics of fluid-solid systems.", *Ind. Eng. Chem.*, 41, 1099-1104.

9. Furkawa, J. & Ohmae, T. (1958). "Liquidlike behaviour of fluidized particles." *Ind. Eng. Chem.*, 50, 821-828.

10. Schügerl, K. Merz, M. & Fetting, F. (1961). "Rheologische Eigenschaften von gasdurchströmten Fliessbettsystemen." *Chem. Eng. Sci.*, 15, 1-38.

11. Barenblatt, G. I. (1996) *Scaling, self-similarity, and intermediate asymptotics*, Cambridge University Press

12. Davidson, J. F. & Harrison, D. (1963). *Fluidised particles*, Cambridge University Press.

13. Rhodes (1998). *Introduction to Particle Technology*, chap. 5. Wiley.

The 12th International Conference on Fluidization - New Horizons in Fluidization Engineering, Art. 106 [2007]